



6 CRAIOVA 8-9 CHIȘINĂU

SIELMEN

OCTOBER 2015

PROCEEDINGS

OF THE 10th INTERNATIONAL CONFERENCE
ON ELECTROMECHANICAL AND POWER
SYSTEMS

ISBN 978-606-567-284-0

Organized by

FACULTY OF POWER AND ELECTRICAL ENGINEERING OF CHIȘINĂU -
MOLDOVA

FACULTY OF ELECTRICAL ENGINEERING OF CRAIOVA - ROMANIA
FACULTY OF ELECTRICAL ENGINEERING OF IASI – ROMANIA

Printed with the support of



Editura ALMA

Applied informatics and intelligent systems

1	Fuzzy Controllers for Variable Speed Pump Control	<i>Daniela Popescu, Jenica-Ileana Corcău</i>	81
2	Charge-discharge optimization of rechargeable battery pack	<i>Constantin Daniel Oancea, Florin Călin</i>	86
3	On Multi-motor Control by a Single Microcontroller and a VHL Programming Language. The Software Design.	<i>Dan Mihai</i>	90
4	On Multi-motor Control by a Single Microcontroller and a VHL Programming Language. The Hardware Platform.	<i>Dan Mihai</i>	96
5	Effective diagnosis for vitiligo skin disease a neural network approach	<i>Viviana Mihaela Bostan, Brândușa Pantelimon</i>	102
6	Improving of 2-D FEM Modeling of a SMES Device Using the Response Surface Methodology Applied on 3-D FEM Modeling	<i>Alin-Iulian Dolan, Florian Ștefănescu</i>	108
7	Power Monitoring System with Wireless Connectivity for Legacy PLC based Systems	<i>Cristian-Gyözö Haba, Liviu Breniuc</i>	114
8	Predictive Technique Applied in Induction Motor Drives	<i>Sergiu Ivanov, Vladimir Răsvan, Eugen Bobașu, Dan Popescu, Florin Știngă</i>	118
9	Tuning the Parameters for the DWT Analysis of Waveforms Acquired from a Power Plant	<i>Ileana-Diana Nicolae1, Petre-Marian Nicolae2, Dinuț-Lucian Popa2, Ionuț Smărândescu2</i>	122

Automations & robots

1	Analytical Algorithms for Synthesis of the State Space Controllers for the Control Systems with Aperiodic Step Response	<i>Ion Fiodorov, Bartolomeu Izvoreanu, Irina Cojuhari, Dumitru Moraru</i>	131
2	A Hybrid Petri Net Model for a Packing System	<i>Mircea-Adrian Drighiciu, Constantin Daniel Cismaru</i>	137

Biomedical Engineering

1	System for medical data acquisition and patient health state telemonitoring	<i>Lucian Niță, Lenuța Alboaie</i>	145
2	Influence of Non-Homogeneities of the Nerve Fibers Located Inside the Spinal Cord upon their Activation Threshold	<i>Laura Darabant, Mihaela Crețu, Radu Ciupa</i>	149
3	The Development and Tests of a New Hybrid FES-Exoskeleton Upper Limb Assisting Device for Disabled Patients	<i>Serea Florin, Hartopanu Sergiu, Poboroniuc Marian, Irimia Dănuț</i>	152

Electrical apparatus

1	Design and 2D Numerical Modeling of a Single Phase AC Inductors with Ferromagnetic Core	<i>Ioan Popa, Alin-Iulian Dolan, Constantin Florin Ocoleanu</i>	161
---	---	---	-----

Electrical energy transport and distribution

1	Mathematical Model of Flexible Alternating Current Link Based on Phase-Shifting Transformer with Circular Rotation of the Phase Angle.	<i>Valeriu Boșneagă, Victor Suslov, Vitaly Postolaty</i>	171
2	Operating Reliability Evaluation of Distribution Networks 10 kV	<i>Victor Popescu</i>	177

Design and 2D Numerical Modeling of a Single Phase AC Inductors with Ferromagnetic Core

Ioan Popa, Alin-Iulian Dolan and Constantin Florin Ocoleanu

University of Craiova, Faculty of Electrical Engineering, Craiova, Romania, ipopa@elth.ucv.ro, adolan@elth.ucv.ro

Abstract— This paper proposes a more accurate design of a single-phase AC current inductors with ferromagnetic core, for given values of inductance, of peak value of current and of magnetic flux density. The procedure combines an analytical computation design method (analytical model) with a numerical analysis by FEM (numerical model) using QuickField and FEMM software. The analytical model has two components, one considering the ideal coil (without loss) and another component considering real coil (with iron loss). The numerical model also has two components, one magnetic (AC Magnetic Problem) which determines the value of inductance and another component consists of a thermal model (Steady-State Heat Transfer Problem) which determines the temperature distribution in the electromagnetic device. In the magnetic model was considered a constant permeability, but both software allow a nonlinear computation

Keywords—inductors with ferromagnetic core; design; numerical modeling; magnetic and thermal analysis

I. INTRODUCTION

The names of reactors (inductors) or coil inductance are assigned to the passive elements of an electrical circuit or of a power system which in quasi-stationary regime are considered as having only an inductive reactance neglecting the resistance. Reactance coils are used for capacitive reactive power compensation in electric networks (connected in derivation), for short-circuit current limiting in electric network (connected in series) to limit starting currents of asynchronous motors, for harmonic filtering of AC current or for smoothing rectified current, for neutral grounding of power networks and to protect against overvoltage [1]. Depending on destination, the reactance coils are made with ferromagnetic core or in air (without ferromagnetic core), single- or three-phase, it can be dry or in oil, resin or beton embedded.

Controlling of the reactive power of the inductor coils for balancing the capacitive reactive power is performed by adjusting the inductance which is obtained by changing the number of turns of the coil, by changing the air gap or by changing the permeability of the magnetic core. The reactance of the inductors connected in series has to rest constant for large changes in the current and for this reason they are made in air (non-ferromagnetic core). The coil inductors used in the harmonic filters construction operate for limited values of the current and they are made with ferromagnetic core.

The inductors with ferromagnetic core are provided with an air gap which interrupts the continuity of the magnetic circuit. The presence of the air gap determines

the reduction of the magnetic remanence and lead to increasing the current required to obtain a maximum value of the magnetic flux density. On the other hand, the air gap has the role of linearizing the magnetization characteristic (magnetic flux versus the current intensity). Single-phase filtering inductors used in DC power circuits have values of mH order. For protection of AC circuits are used single- or three-phase inductors with ferromagnetic core or single-phase inductors in air (of μH order values). In this paper are considered the AC ferromagnetic core inductors [2].

II. APPROXIMATE CALCULATION OF IDEAL COIL (LOSSLESS)

A. Analytical Model for Ideal Coil

We consider an inductor coil with the magnetic circuit of type E-I (fig. 1) made on grain oriented electrical steel. The known quantities are usually the magnetic flux density (peak value), the self-inductance, the maximum current (being the RMS value) and the maximum current density (peak value) having sinusoidal variations. The problem is to determine the number of turns, the dimensions of the magnetic circuit and of the air gap so that the inductor coil has the required inductance in the given conditions (the magnetic flux density in the magnetic core and the coil conductor must supports the maximum current in order to not exceed the maximum temperature corresponding to the adopted temperature class of electric insulator).

For the problem defined above does not exist a unique solution and, therefore, we try to optimize the geometrical dimensions such that the coil must fill the entire window with the surface (Fig. 1). The width of the window is considered as the determining dimension. The other geometric dimensions are related to the determining dimension by relationships

$$a_1 = k_1 f \quad a = k_2 f \quad h = k_3 f \quad b = k_4 a. \quad (1)$$

First one considers the following values for the coefficients k_1, k_2, k_3, k_4

$$k_1 = 1 \quad k_2 = 2 \quad k_3 = 3 \quad k_4 = 1. \quad (2)$$

such as the magnetic circuit is defined only by one dimension .

The ranges of values of these coefficients may result from an optimization calculation. The average length of a field line, given the above relationships, is $l_m = 13 f$. The magnetic circuit is assumed unsaturated with a constant relative permeability μ_r , without magnetic flux leakage

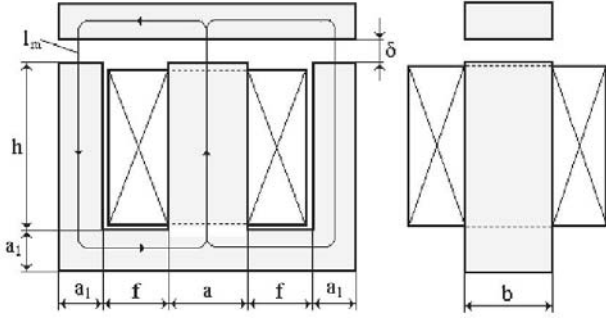


Fig. 1. The dimensions of the coil inductor with iron core of E - I type.

and without iron losses. Under these conditions, we can write the relationship

$$B_{\max} = \mu_r \mu_0 H_{\max} . \quad (3)$$

The above relationship is valid if $B_{\max} \leq 1.2$ T for grain oriented electrical steel and $B_{\max} \leq 0.3$ T for ferrites.

For the air gap, must be taken into account the fringing fields, such that the air gap section S_δ is greater than the core section, which becomes

$$S_m = k_r \cdot (2f)^2 . \quad (4)$$

where k_r is the coefficient for reduction of the useful section of the magnetic core ($0.8 \leq k_r \leq 1$) and the air gap section is about [5]

$$S_\delta = (2f + 4\delta)^2 . \quad (5)$$

where δ is the length of the air gap.

The maximum values of magnetic flux density in the air gap $B_{\delta\max}$ and in the core B_{\max} are linked by magnetic flux conservation relationship

$$B_{\delta\max} S_\delta = B_{\max} S_m . \quad (6)$$

Applying Kirchoff's second theorem in a loop of the magnetic circuit in Fig. 2 results

$$NI_{\max} = H_{\max} l_m + 2\delta H_{\delta\max} = \frac{B_{\max}}{\mu_r \mu_0} l_m + 2\delta \frac{B_{\max} S_m}{\mu_0 S_\delta} . \quad (7)$$

Using the flux method, the inductance of the magnetic circuit can be written as

$$L = \frac{NB_{\max} S_m}{I_{\max}} . \quad (8)$$

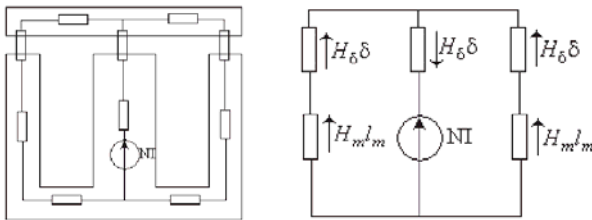


Fig. 2. Reluctances of magnetic circuit and simplified equivalent scheme

and taking into account the relationship (7) we have

$$L = \frac{\mu_0 N^2 S_m}{\frac{l_m}{\mu_r} + 2\delta \frac{S_m}{S_\delta}} . \quad (9)$$

From (7) the number of turns results

$$N = \frac{B_{\max}}{\mu_0 I_{\max}} \left(\frac{l_m}{\mu_r} + 2\delta \frac{S_m}{S_\delta} \right) . \quad (10)$$

and from (9) results the magnetic core section

$$S_m = \frac{L}{\mu_0 N^2} \left(\frac{l_m}{\mu_r} + 2\delta \frac{S_m}{S_\delta} \right) . \quad (11)$$

Substituting N by its expression from (10) results

$$S_m = \frac{\mu_0 L I_{\max}^2}{B_{\max}^2 \left(\frac{l_m}{\mu_r} + 2\delta \frac{S_m}{S_\delta} \right)} . \quad (12)$$

From (4) is obtained

$$f = \frac{1}{2} \sqrt{\frac{S_m}{k_r}} . \quad (13)$$

Based on relationships (1) - (13) has developed a computer program according to the algorithm represented by flowchart of Fig. 3. To reduce magnetic core section should be chosen as big as values for B_{\max} and δ . After calculating the number of turns we need to check if the area occupied by the coil S_{cu} is less than or very close to the magnetic circuit window section S_f , i.e.

$$S_{cu} = \frac{NI_{\max}}{J_{\max} k_u k_i} \leq 3f^2 . \quad (14)$$

where k_u is the filling factor of the winding ($0.3 \leq k_u \leq 0.9$) that depends on the diameter of winding wire and $k_i = I_{\max} / I_{\text{eff}}$, I_{eff} is the current RMS value ($k_s = 0.9$, $k_u = 0.5$, $k_i = 1.41$, $B_{\max} = 1$ T, $J_{\max} = 3.5$ A/mm², $\mu_r = 2000$).

III. APPROXIMATE CALCULATION OF THE REAL COIL (WITH LOSSES)

A. Analytical Model for Real Coil

In the magnetic core there are iron losses (hysteresis and eddy current). The manufacturers of grain oriented electrical steel provide curves showing the evolution of the losses in iron depending on frequency f_c and maximum value of magnetic flux density B_{\max} (in W/kg). In these circumstances we need to know the angle iron loss α (the phase angle between current and magnetic flux) to calculate the magnetizing component of current. We suppose that all quantities are sinusoidal and the known data are maximum values of magnetic flux density B_{\max} , of the current I_{\max} , of the current density J_{\max} and the self inductance of the coil [5], [6], [7].

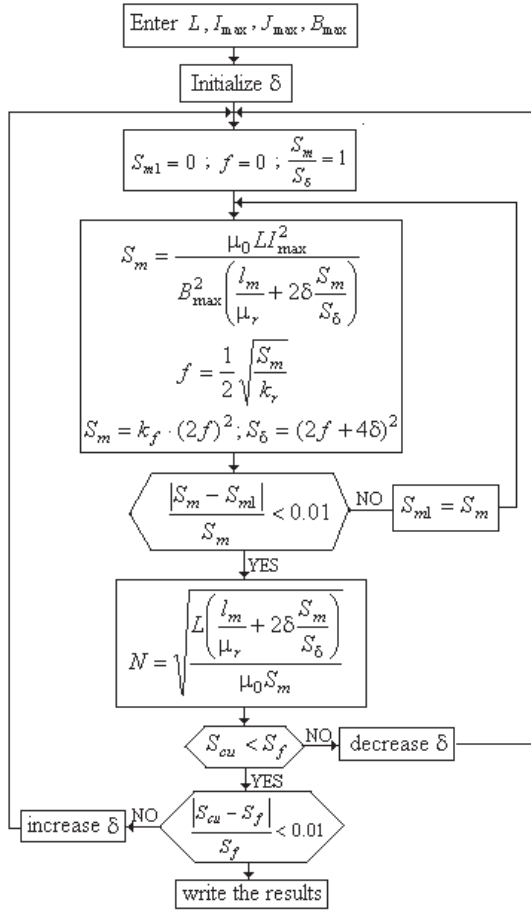


Fig. 3. Flowchart of computation of an ideal inductor coil (lossless).

Supply voltage of coil is written according Boucherot formula as follows

$$U = 4.44 f_c N B_{\max} S_m \square. \quad (15)$$

Considering (7) we can write relationship

$$NI = \frac{B_{\max}}{\sqrt{2}\mu_0} \left(\frac{l_m}{\mu_r} + 2\delta \frac{S_m}{S_\delta} \right). \quad (16)$$

Apparent power S of coil (in VA) is written as (with the approximation of Kapp which neglects the coil resistance and the leakage inductance, see Fig. 4 and Fig. 5)

$$S = UI = \frac{4.44}{\sqrt{2}\mu_0} B_{\max}^2 S_m f_c \left(\frac{l_m}{\mu_r} + 2\delta \frac{S_m}{S_\delta} \right). \quad (17)$$

From equation (17) finds that the apparent power of the coil may be increased by

- Increasing the cross-section area of magnetic circuit S_m ;
- Increasing the maximum magnetic induction B_{\max} ;
- Increasing the air gap δ .

The increasing of S_m and B_{\max} has the effect on increasing of the volume coil and of the iron losses. Therefore increasing the air gap δ is an advantageous solution, resulting also the linearization of magnetization characteristic.

The iron losses are written as [4], [5], [6], [7], [8]

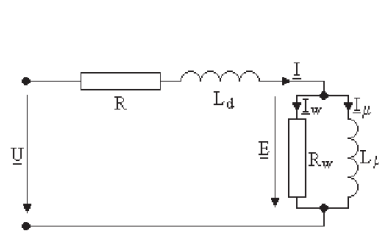


Fig. 4. The electrical equivalent full schema (R and L_d are absent in the approximation of Kapp).

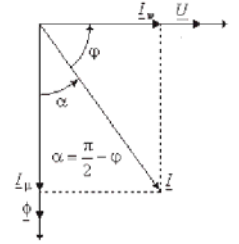


Fig. 5. Fresnel diagram relative to the iron core coil in sinusoidal approximation.

$$P_{fe} = k_H V_m f_c B_{\max}^\eta + k_F V_m f_c^2 B_{\max}^2. \quad (18)$$

where $V_m = S_m l_m$ and replacing the term $V_m f_c B_{\max}^2$ considering (17) results the relationship of iron losses

$$P_{fe} = \frac{\sqrt{2}\mu_0}{4.44} UI \left(k_H B_{\max}^{\eta-2} + k_F f_c \right) \frac{l_m}{\frac{l_m}{\mu_r} + 2\delta \frac{S_m}{S_\delta}}. \quad (19)$$

This relationship shows that the iron loss decreases when the air gap increases. On the other hand the iron losses correspond almost entirely with active power $P = UI \sin(\alpha)$ absorbed by the coil and thus results the loss phase angle α

$$\alpha = \arcsin \left(\frac{\sqrt{2}\mu_0}{4.44} \left(k_H B_{\max}^{\eta-2} + k_F f_c \right) \frac{l_m}{\frac{l_m}{\mu_r} + 2\delta \frac{S_m}{S_\delta}} \right). \quad (20)$$

The coefficients k_H and k_F are calculated from the curves provided by the manufacturer (common values are $k_H = 55$, $k_F = 0.78$, $\eta = 1.6$).

The reactive component of current $I_r = I \cos(\alpha)$ is used in calculation of the cross-section of magnetic core and in determination of quantity f (Fig. 1).

Based on the equations (15) - (20), the flowchart in Fig. 3 has been modified to obtain the geometry of the coil, the magnetic circuit size and the number of turns taking into account the iron core losses.

IV. ANALYTICAL RESULTS

With the developed programs were plotted the curves shown in Fig. (6-10). Figure 6 shows the evolution of determining dimension f depending on the value of the inductance in the range (0.1-200) mH for different values of current and for the magnetic flux density of 1 T and Fig. 7 shows the evolution of the air gap.

In Fig. 8-9 we present a comparison of the evolution of the determining dimension and of the air gap versus the inductance in the case of ideal and real coil. It finds that the size of the magnetic core and the air gap is smaller in the case of the real coil.

Number of turns of the coil, resulting from the analytical model is lower for real coil (Fig. 10).

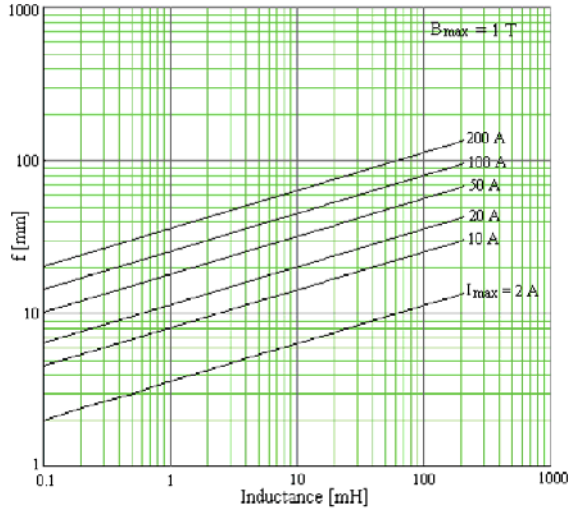


Fig. 6. Evolution of the determining dimension versus the inductance value and versus the maximum current in the for the ideal coil.

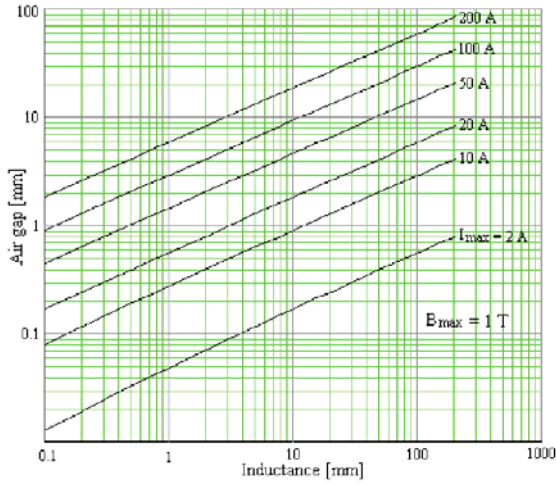


Fig. 7. Evolution of the air gap versus the inductance value and versus the maximum current in the for the ideal coil.

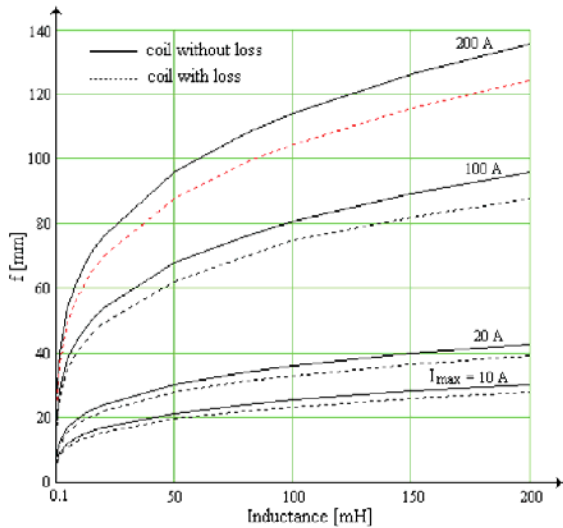


Fig. 8. Comparison concerning the evolution of determining dimension versus inductance and versus maximum current for ideal and real coil.

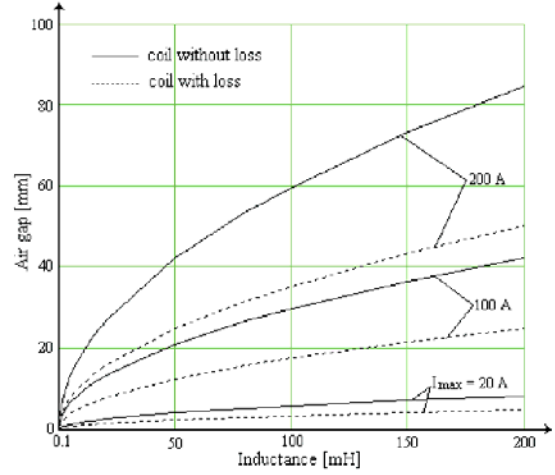


Fig. 9. Comparison concerning the evolution of air gap versus inductance and versus maximum current for ideal and real coil.

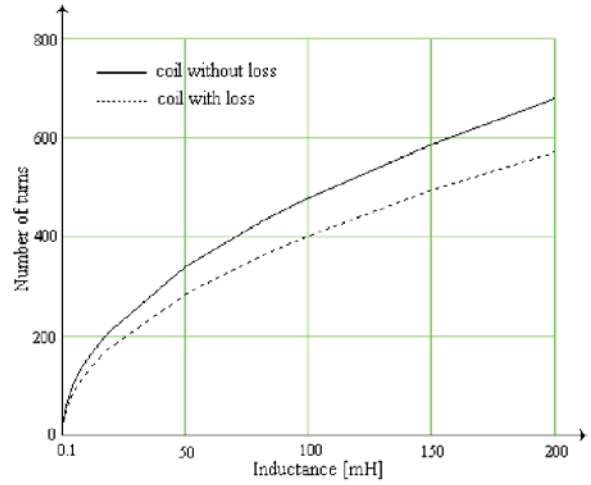


Fig. 10. Comparison concerning the evolution of the turns number versus the inductance for ideal and real coil

V. 2D NUMERICAL MODELS

The approximate calculations of the ideal and real coil provide the geometric dimensions of the magnetic circuit and coil data (number of turns and diameter of the conductor). These data helps to develop the magnetic numerical model which allows a more accurately determination of the coil inductance. The numerical value of inductance does not match with that imposed in the approximate calculation. The magnetic numerical models were obtained using QuickField and FEMM software [11], [12].

A. Magnetic numerical model equation

The equation for the analysis of AC magnetic field is

$$\frac{\partial}{\partial x} \left(\frac{1}{\mu} \frac{\partial A}{\partial x} \right) + \frac{\partial}{\partial y} \left(\frac{1}{\mu} \frac{\partial A}{\partial y} \right) - \sigma \frac{\partial A}{\partial t} = -J_s \quad (21)$$

where A is the magnetic vector potential (z-axis component), μ is the permeability, σ is the electrical conductivity and J_s is the source current density. The field problem is coupled to the coil circuit.

B. Thermal numerical model equation

The equation governing the thermal field analysis in steady state is

$$\frac{\partial}{\partial x} \left(\lambda \frac{\partial T}{\partial x} \right) + \frac{\partial}{\partial y} \left(\lambda \frac{\partial T}{\partial y} \right) + S = 0. \quad (22)$$

where T is the absolute temperature, λ is the thermal conductivity and S is the source term (the sum of joule losses in the coil and iron losses).

To develop the numerical model must be known the specific electric heat sources in the coil and also the specific heat sources in magnetic core. The specific electric losses (by Joule effect, in W/m^3) is calculated using the relationship

$$p_e = \rho J_m^2. \quad (23)$$

where ρ is the electric resistivity, $J_m = I / S_c$ is an average current density value in cross-section area of conductor (RMS value) and S_c is the cross section area of the conductor.

The specific losses in the magnetic core (iron losses in W/m^3) is calculated using the relationship [10]

$$p_m = C_m \left(\frac{f_c}{50} \right)^\alpha \cdot \left(\frac{B_m}{1.5} \right)^\beta \cdot \gamma. \quad (24) \square$$

where B_m is the average value of magnetic flux density in the core provided by QuickField, $C_m = 1.5$ [W/kg] is a material constant and $\alpha = 1$, $\beta = 2$ are constants.

C. Correction of the turns number of coil

The numerical values of inductance from QuickField or FEMM are higher than those imposed in analytical calculation, the error is smaller for real coil (Tables I and II). To obtain the desired inductance there are the following possibilities:

- Changing the air gap value;
- Changing the size of the magnetic core;
- Changing the number of turns.

The fastest and most economical solution is to reduce (in this case) number of turns of the coil. Considering that the inductance coil is proportional to the square of the number of turns, the corrected number of turns N_c is

$$N_c = N \sqrt{\frac{L_f}{L_i}}. \quad (25)$$

where N is the initially number of turns resulted from the analytical model, L_i is the initial inductance resulted from the numerical model L_f is the final inductance of the coil resulting from a numerical model with corrected number of turns.

VI. NUMERICAL RESULTS

The magnetic numerical model has been developed both in QuickField and in FEMM. The figure 11 shows the spectrum of magnetic flux density. The table I (coil without losses) and table II (coil with losses) present four inductance values for different current values, the analytical values of the inductance and of the number

turns and the corrected number of turns. Inductance value was calculated using the flux method and energy method (the marked values in tables I and II by *). The corrected number of turns N_c marked with "+" corresponds to the numerical model performed in FEMM. In Fig. 10 is shown the variation of magnetic flux density (peak value) on sections AB and CD (Fig. 11).

The Table III shows the contribution of each zone of computational domain (Fig. 11) related to total inductance of the electromagnetic device. It finds that the most important contribution (90.71%) has the coil window area and the air gap area. It can not be neglected the outside zone of device area bordered by boundary of computing domain (7.93%). Contribution of air gap on inductance value is almost 50%, which largely justify the differences arising between analytical values of inductance and numerical values.

The figure 14 shows the temperature distribution in the electromagnetic device. If a lower maximum temperature is imposed, then the analytical model needs a lower current density.

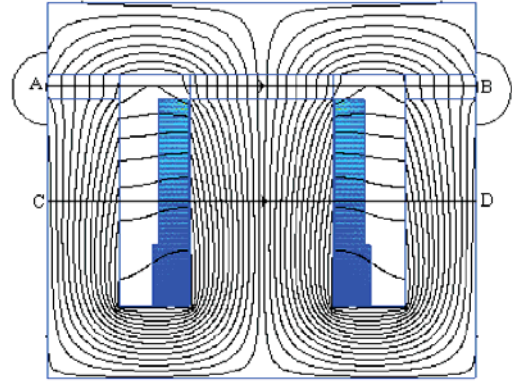


Fig. 11. Distribution of magnetic flux density ($L = 100$ mH, $I_{\max} = 200$ A).

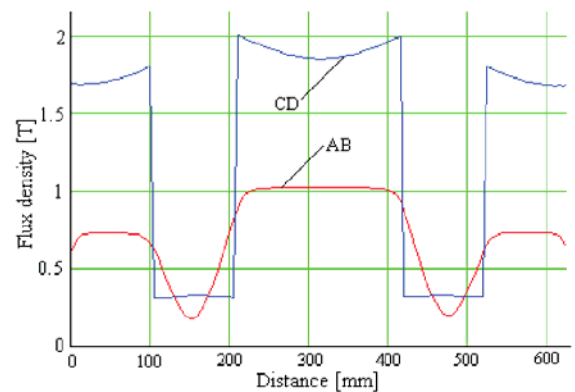


Fig. 12. Variation of magnetic flux density (peak value) on the sections AB and CD (Fig. 11).

The numerical models were indirectly experimentally validated on a no load single-phase transformer (600 VA) with 9.98% error for inductance value. This error is justified by the fact that the leakage flux from frontal areas of the coil is not taken into account in 2D numerical model.

TABLE I.
INDUCTANCE VALUES OBTAINED WITH NUMERICAL MODEL BEFORE
AND AFTER CORRECTION OF TURNS NUMBER (IDEAL COIL)

Analytical model					Numerical model		
L [mH]	I_{max} [A]	N	L_i [mH] QF	L_i [mH] FEMM	N_c	L_f [mH] QF	L_f [mH] FEMM
200	200	676	728.61 727.06*	718.62	354 356 ⁺	205.56 205.23*	199.32 199.32*
100	200	479	332.02 331.5*	324.43	264 266 ⁺	101.29 101.16*	100.06 100.06*
10	100	152	21.1 20.97*	21.04	103 103 ⁺	10.05 9.99*	9.92 9.92*
1	10	48	1.47 1.46*	1.46	40 40 ⁺	1.017 1.015*	1.01 1.01*

TABLE II.
INDUCTANCE VALUES OBTAINED WITH NUMERICAL MODEL BEFORE
AND AFTER CORRECTION OF TURNS NUMBER (REAL COIL)

Analytical model					Numerical model		
L [mH]	I_{max} [A]	N	L_i [mH] QF	L_i [mH] FEMM	N_c	L_f [mH] QF	L_f [mH] FEMM
200	200	570	571 570*	563.72	340 340 ⁺	203.88 203.19*	200.58 200.58*
100	200	403	252.3 251.48*	256.1	252 252 ⁺	102.17 101.85*	100.14 100.14*
10	100	126	18.19 18.04*	18.06	94 94 ⁺	10.31 10.28*	10.05 10.05*
1	10	36	1.39 1.38*	1.38	34 34 ⁺	0.998 0.989*	0.998 0.998*

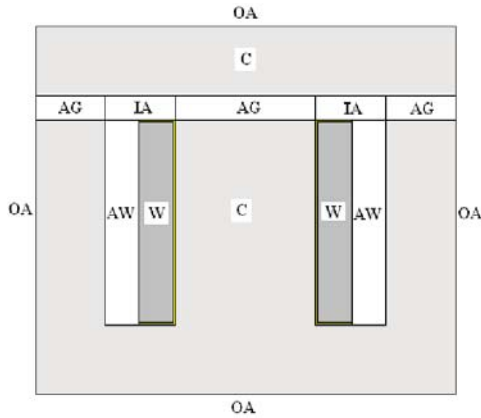


Fig. 13. Subdomains that contribute to the total inductance of the inductor coil, AG – air gap, C – ferromagnetic core, W – winding +insulation, AW –air window, IA – indoor air, OA – outdoor air.

TABLE III.
INDUCTANCE VALUES BY SUBDOMAINS (REALCOIL)

Subdomain	Magnetic field energy [J]	Inductance [mH]	Percentage [%]
AG	497.3	49.73	48.736
C	13.931	1.39	1.36
W	173.33	17.33	16.98
AW	173.47	17.347	17
IA	81.499	8.15	7.98
OA	80.899	8.09	7.93
W+AW+AG+IA	925.6	92.56	90.71
W+AW+AG+IA+C	939.53	93.95	92.07

W+AW+AG+IA+C+OA	1020.4	102.04	100
-----------------	--------	--------	-----

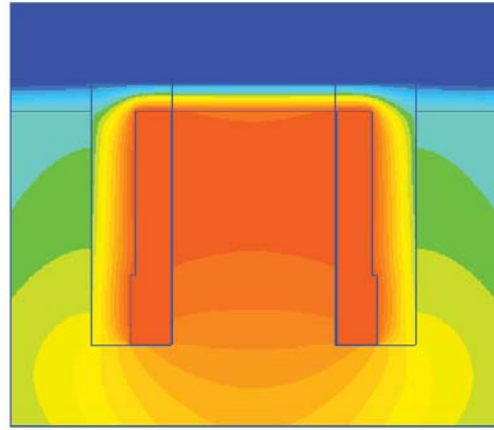


Fig. 14. Temperature distribution in electromagnetic device ($L = 100$ mH, $I_{max} = 200$ A, $T_a = 313$ K (40 °C), $T_{max} = 395$ K (122 °C)).

Inductance calculated by the numerical model is less than that determined by experiment (winding applied voltage, current in the coil and coil resistance).

The thermal numerical model took into account the transferred heat by the frontal surfaces with a greater heat transfer coefficient. The real heat transfer coefficient is multiplied by a coefficient defined by the ratio of the surfaces that are not borders but that transfer the heat and the borders surfaces.

VII. CONCLUSIONS

The study shows that the analytical presented model which neglects the leakage flux offer the geometrical data and the turns number which give an inductance value experimentally non validated. The errors are smaller for real coil but enough great (30 - 100%) increasing with the inductance value. This conclusion is validated by numerical models developed in QuickField and FEMM, the errors between these being less than 1%. The numerical models were experimentally validated on a single-phase transformer. Fine adjusting of inductance value can be achieved by adjusting the air gap. The procedure presented can be improved considering nonlinearity of magnetic core and using a 3D numerical model.

In order to optimize the geometry of the device must be carried out and a numerical modeling study using the equation of electric circuit and the equation of magnetic circuit under assumptions of current source supply and takings into account the magnetic saturation and hysteresis cycle.

REFERENCES

- [1] C. Bălă, L. Țogui and M. Covrig, "Reactor for energy systems," (in roumanian).Technica Edition, Bucharest, 1982.
- [2] E. Lăzărescu and I. Potârniche, "Dry transformer. Reactors. Design. Applications," (in roumanian), AGIR, Edition, Bucharest, 2011.
- [3] P. L. Kalantarov and L. A. Teitlin, "Inductances Calculation," (in roumanian), Editura Tehnică, București, 1958.
- [4] A. Timotin, V. Hortopan, A. Ifrim and M. Preda, "Lessons of Theoretical Electrical Engineering," (in roumanian), EDP, București, 1970.
- [5] F. Leplus, "Bobine à noyau de fer en régime variable," Techniques de l'ingénieur, Edition TI, réf. D-3010, Février 2007.

- [6] M. Piou, "Electrotechnique - Chapitre 4 Inductances et bobines," <http://public.iutenligne.net/electricite/piou/magnelecpro/MagnElecPro/>, 2010.
- [7] M. Jufer, "Circuits magnétiques – Exemples et applications, Techniques de l'ingénieur," Edition TI, réf. 1051, Février 2007.
- [8] C. Mocanu, "Electromagnetic Field Theory," (in roumanian), Edition D&P, București, 1981.
- [9] Ziwei Ouyang, Juan Zhang and William Gerard Hurley, "Calculation of Leakage Inductance for High Frequency Transformers," IEEE Transactions on Power Electronics, vol. 30, No. 10 October 2014, pp. 5779 – 5775.
- [10] Peng Li, Guoqiang Huang, Liqiang Xie and Xiaojing Hu, "Research on Calculating Leakage Inductance of Power Transformer and its Application to Winding Deformation Analysis," CICED 2008, Technical session 1, Distribution network equipment, pp. 1-7.
- [11] Tera Analysis Ltd. QuickField Software, version 5.10 Professional, <http://quickfield.com>, 2014.
- [12] D. Meeker, Finite element method magnetics, version 4.2, <http://www.femm.info/wiki/HomePage>, 2013.